

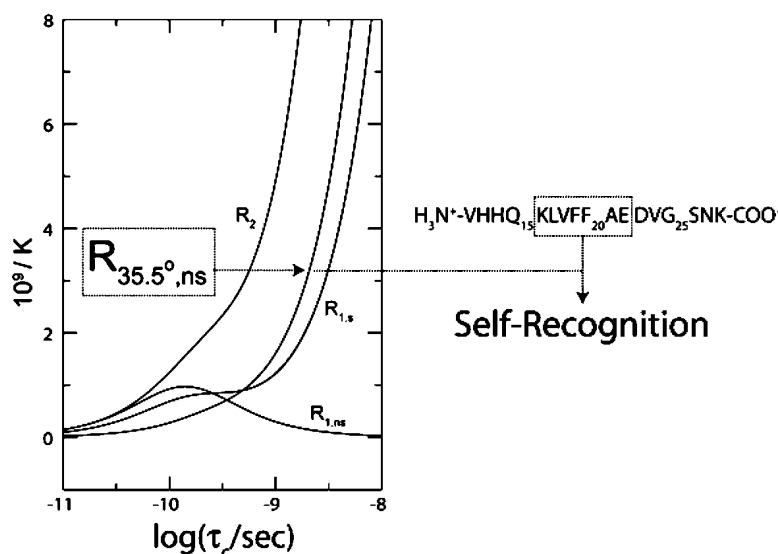
Communication

Mapping Polypeptide Self-Recognition through H Off-Resonance Relaxation

Veronica Esposito, Rahul Das, and Giuseppe Melacini

J. Am. Chem. Soc., **2005**, 127 (26), 9358-9359 • DOI: 10.1021/ja051714i • Publication Date (Web): 09 June 2005

Downloaded from <http://pubs.acs.org> on March 25, 2009



More About This Article

Additional resources and features associated with this article are available within the HTML version:

- Supporting Information
- Links to the 2 articles that cite this article, as of the time of this article download
- Access to high resolution figures
- Links to articles and content related to this article
- Copyright permission to reproduce figures and/or text from this article

[View the Full Text HTML](#)

Mapping Polypeptide Self-Recognition through ^1H Off-Resonance Relaxation

Veronica Esposito, Rahul Das, and Giuseppe Melacini*

Departments of Chemistry, Biochemistry and Biomedical Sciences, McMaster University, 1280 Main Street W., Hamilton, Ontario L8S 4M1, Canada

Received March 17, 2005; E-mail: melacin@mcmaster.ca

Amyloid fibril formation is associated with several neurodegenerative disorders either through a gain in toxic function or through a loss of function.¹ The prefibrillar soluble oligomers have been shown to be significantly more toxic than the mature amyloid fibrils, as these early aggregates lead to apoptotic or necrotic cell death by causing oxidative stress and altered cellular homeostasis as a result of their interactions with membranes.^{1,2} Solution studies help understand the mechanism of formation of the soluble toxic oligomeric intermediates, and they may provide clues for the inhibition of the early, still reversible, steps in the cascade of events that lead to cell death. However, the molecular basis underlying these initial self-recognition processes in solution is not fully understood. ^1H NMR relaxation rates provide a widely applicable and sensitive probe ideally suited to investigate the weak ($K_D \sim$ micromolar to millimolar range) interactions that frequently mediate polypeptide oligomerization. Specifically, the NMR relaxation rates that are most sensitive to the formation of high molecular weight oligomers are those which increase monotonically with increasing correlation time, τ_c . This is the case for the ^1H transverse (R_2) and the selective ^1H longitudinal ($R_{1,s}$) relaxation rates because both R_2 and $R_{1,s}$ contain a spectral density term calculated at zero frequency that results in the desired direct τ_c dependence (Figure 1a).^{3–5} However, the measurement of both R_2 and $R_{1,s}$ is often experimentally challenging.³ The accurate determination of ^1H R_2 rates by CPMG sequences ($90_x^\circ - (\tau - 180_y^\circ - \tau)_{2n}$) is hampered by the concurrent homonuclear scalar coupling (J^{HH}) evolution, and the measurement of ^1H $R_{1,s}$ rates is limited only to very small ligands with well-resolved NMR resonances for which selective inversions can be implemented. In addition, even when the necessary selectivity is obtained, multiple selective measurements on different protons are required to produce a full interaction map. Here, we propose a different NMR experiment based on nonselective ^1H off-resonance relaxation that avoids the drawbacks intrinsic to the measurement of both ^1H R_2 and $R_{1,s}$. The proposed method has been applied to the peptide A β (12–28) with sequence $\text{H}_3\text{N}^+ - \text{V}_{12}\text{HHQKLVFFAEDVGSNK}_{28} - \text{COO}^-$ dissolved in acetate buffer (pH 4.7), which has been shown to provide a reproducible model for the early stages of the reversible oligomerization preceding the formation of amyloid deposits linked to Alzheimer's disease.⁶

The proposed relaxation experiment is implemented through an off-resonance spin-lock with a typical trapezoidal shape that ensures adiabaticity.⁷ This trapezoidal relaxation block is inserted after the interscan delay and before the first 90° pulse of a 1D or 2D pulse sequence (i.e., TOCSY)^{8–11} used to detect the signal and to monitor the decay during the off-resonance spin-lock (Figure 2). It is easily shown (Supporting Information) that for a given spin i the initial rate of decay along the effective field tilted by an angle θ with respect to the longitudinal axis of the rotating frame is

$$R_{\theta,ns}^i = (c - 1)cR_{1,ns}^i + s^2R_2^i \quad (1)$$

where $c = \cos(\theta)$, $s = \sin(\theta)$, $R_{1,ns}$ and R_2 are the nonselective

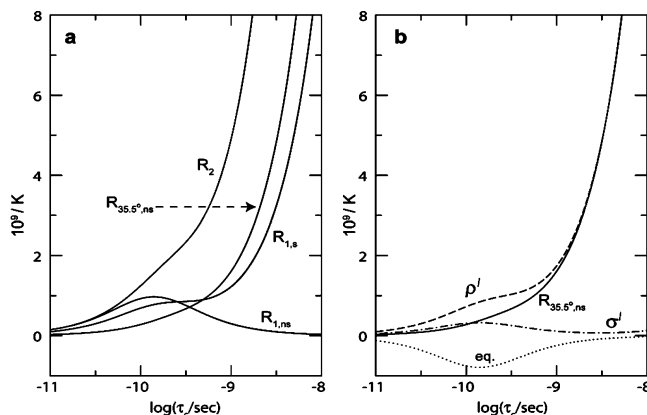


Figure 1. Plot of relaxation rates as a function of the correlation time (τ_c) for a model two-spin system. The proton Larmor frequency is 700 MHz and $K = \hbar^2\gamma_{\text{H}}^4/10r_{ij}^6$. (a) The τ_c dependence of the nonselective ($R_{1,ns}$) and selective ($R_{1,s}$) longitudinal relaxation rates as well as of the transverse relaxation rate for in-phase magnetization (R_2) and of the nonselective off-resonance relaxation rate at the tilt angle $\theta = 35.5^\circ$ ($R_{35.5^\circ,ns}$). (b) The τ_c dependence of the self- (ρ'), cross-relaxation (σ'), and equilibrium ($-\cos(35.5^\circ)R_{1,ns}$) components of $R_{35.5^\circ,ns}$. Further details are available in the Supporting Information.

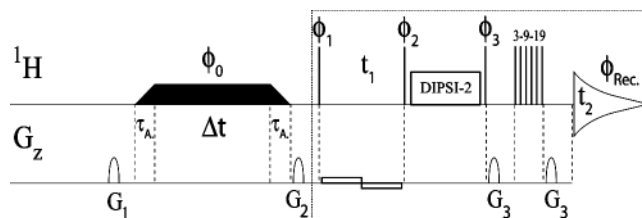


Figure 2. Pulse sequence for the off-resonance TOCSY experiment. The off-resonance spin-lock has a trapezoidal shape including two adiabatic pulses of duration $\tau_A = 4$ ms, which scale linearly up/down to/from a field with a strength (ω_1) of 8.23 kHz and duration Δt . The frequency offset is $\Delta\nu = \omega_1/\tan(\theta)$, where θ is the tilt angle of the effective field.⁷ Summation of data acquired with positive and negative offsets in alternate scans is employed to minimize angular dispersion.⁸ Water suppression was achieved through a 3–9–19 Watergate spin-echo.⁹ A weak bipolar gradient¹⁰ was implemented during the incremented delay t_1 to suppress radiation damping, which would otherwise deteriorate the effectiveness of the Watergate water suppression. The phase cycle is $\phi_0 = x$; $\phi_1 = x, x, -x, -x$; $\phi_2 = (x)_8, (-x)_8$; $\phi_3 = (x)_4, (-x)_4$; $\phi_{\text{Rec}} = x, x, (-x)_4, x, x, -x, -x, (x)_4, -x, -x$; the DIPSI-2¹¹ phases are $-y, y$, and the 3–9–19 Watergate phases are $x, -x$.⁹ The G_1 , G_2 , and G_3 pulsed field gradients are sine-bell shaped and have a duration of 1 ms followed by a delay of 0.2 ms. G_1 and G_2 purge residual transverse components of the magnetization before and after the off-resonance spin-lock. The relative ratios for the G_1 , G_2 , and G_3 strengths are 17, 11, and 30, respectively. The standard 2D TOCSY in the dotted box can be replaced by a simple 1D experiment in case there is no overlap in the 1D spectrum. Further details are available in the Supporting Information.

longitudinal and transverse (in-phase) relaxation rates (Figure 1a). The tilt angle $\theta = 35.5^\circ$ is particularly interesting because at this θ value, NOE/ROE compensation annihilates the effective cross-

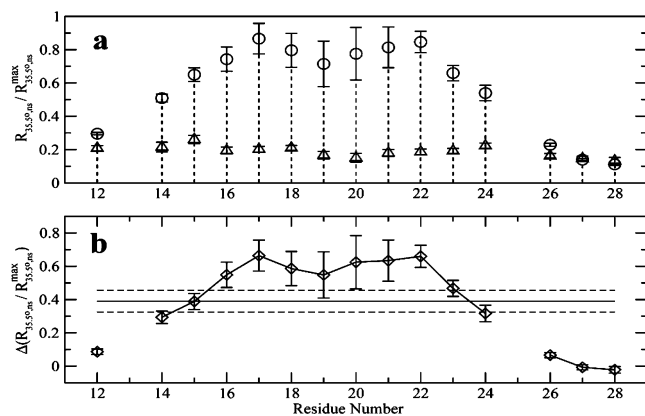


Figure 3. Plot of relative $R_{35.5^\circ,ns}$ relaxation rates versus residue number in $A\beta$ (12–28) with sequence $H_3N^+-VHHQ_{15}KLVFF_{20}AEDVG_{25}SNK-COO^-$. All rates were measured at 20 °C in 50 mM acetate- d_3 buffer pH 4.7 and at 700 MHz. No well-resolved TOCSY cross-peaks were available for H_{13} and G_{25} . (a) Circles and triangles refer to rates at 1 and 0.1 mM $A\beta$ (12–28) concentrations, respectively. All rates are normalized to the maximum rate and smoothed by averaging over a two residue ($i, i + 1$) window (Supporting Information) with the exception of V_{12} , V_{24} , and K_{28} for which no averaging was possible. For these three residues, the actual normalized rates are reported for the sake of completeness. (b) Difference between the two plots shown in panel (a). The horizontal solid and dashed lines indicate the mean \pm the standard error.

relaxation rate (ρ^l) in the spin-diffusion limit⁷ (Figure 1b), therefore minimizing cross-talk effects between different spins and causing the $R_{35.5^\circ,ns}$ rate in the spin-diffusion limit to approach the effective self-relaxation rate at $\theta = 35.5^\circ$ (ρ) (Figure 1b) (Supporting Information). At $\theta = 35.5^\circ$, the contribution from R_2 in eq 1 already significantly prevails over that from $R_{1,ns}$, resulting in the desired marked monotonic increase of $R_{\theta,ns}$ with τ_c (Figure 1a,b). The $R_{35.5^\circ,ns}$ measurement is not limited by the selectivity requirements typical of R_1 experiments. In addition, the R_2 artifacts arising from J -transfer in CPMG-like pulse trains are here effectively suppressed by placing the spin-lock field off-resonance.⁷ An additional advantage of the proposed experiment (Figure 2) is that multiple TOCSY cross-peaks are available to monitor the relaxation of each single 1H spin, thus minimizing overlap problems. For instance, when measuring $R_{35.5^\circ,ns}$ rates for $H\alpha$ spins in a polypeptide, if the ($H\alpha,HN$) cross-peaks are not well resolved or are weakened by saturation transfer from water, the ($H\alpha,H\beta$) cross-peaks are often available as alternative probes of the decay.

As an example of the use of the $R_{35.5^\circ,ns}$ rates, we have applied the proposed relaxation experiment (Figure 2) to the peptide $A\beta$ (12–28). The dissociation constant for the $A\beta$ (12–28) oligomerization equilibria has been reported to be in the millimolar range, but the molecular determinants for self-recognition underlying oligomer formation are not fully understood.¹² We therefore prepared two $A\beta$ (12–28) samples, one at 1 mM and one at 0.1 mM, and we measured the $R_{35.5^\circ,ns}$ rates of the $H\alpha$ spins for both samples (Supporting Information). As shown in Figure 3a, for the diluted $A\beta$ (12–28) sample, no significant variations in the measured $H\alpha$ - $R_{35.5^\circ,ns}$ rates are observed throughout the sequence. For G_{25} , no well-resolved TOCSY cross-peaks were available, but it is likely that glycine represents an exception because of its markedly different 1H density around the $H\alpha$ spins. These observations suggest that at least for the $C\beta$ -containing residues of $A\beta$ (12–28), the measured $H\alpha$ - $R_{35.5^\circ,ns}$ rates do not depend significantly on the amino acid type. A significant increase in the $H\alpha$ - $R_{35.5^\circ,ns}$ rates for most residues is, however, observed when the peptide concentration is 10-fold higher (Figure 3a). The difference between $H\alpha$ - $R_{35.5^\circ,ns}$ rates in the concentrated and in the dilute samples

(Figure 3b) shows that the 10-fold increase in concentration results in higher-than-average $H\alpha$ - $R_{35.5^\circ,ns}$ enhancements only for residues $K_{16}LVFFAE_{22}$, suggesting that this region contains key determinants for self-recognition while the flanking residues remain relatively flexible even after oligomerization. The uncertainty in the start and end points of the critical peptide segment is expected to be about ± 1 residue (16 ± 1 , 22 ± 1). This result is fully consistent with previous independent mutation-based studies on full-length $A\beta$ peptides, indicating that residues $K_{16}LVFFA_{21}$ in the central hydrophobic cluster of $A\beta$ serve as a key binding element for $A\beta$ fibrillization.¹³ Furthermore, mutations at E_{22} linked to familial Alzheimer's disease significantly affect $A\beta$ aggregation.¹⁴

In conclusion, we have shown that nonselective off-resonance relaxation rates with $\theta = 35.5^\circ$ ($R_{35.5^\circ,ns}$) are effective probes of noncovalent interactions circumventing the J -transfer and selectivity problems typically associated with transverse and longitudinal relaxation measurements. When applied to $H\alpha$ spins in polypeptides at different concentrations, the proposed experiment is useful to map at residue-resolution self-recognition in the early steps of aggregation, providing a new spectroscopic tool to investigate the molecular determinants of amyloidogenesis. The method is expected to be widely applicable not only to the fast growing family of amyloidogenic peptides,¹⁵ including other forms of $A\beta$ peptides, but also to the screening and mapping of protein–ligand interactions in general.

Acknowledgment. Dedicated to the memory of Prof. Murray Goodman. We thank Dr. A. Bain, H. Huang, and J. Mилоjevic for helpful discussions, NSERC for funding, and the University of Naples for a fellowship to V.E.

Supporting Information Available: Details for Materials and Methods as well as the derivation of eq 1. This material is available free of charge via the Internet at <http://pubs.acs.org>.

References

- (1) (a) Miranker, A. D. *Proc. Natl. Acad. Sci. U.S.A.* **2004**, *101*, 4335. (b) Stefani, M.; Dobson, C. M. *J. Mol. Med.* **2003**, *81*, 678. (c) Zagorski, M. G.; Yang, J.; Shao, H. Y.; Ma, K.; Zeng, H.; Hong, A. *Methods Enzymol.* **1999**, *309*, 189.
- (2) (a) Merlini, G.; Westermark, P. *J. Internal Med.* **2004**, *255*, 159. (b) Temussi, P. A.; Masino, L.; Pastore, A. *EMBO J.* **2003**, *22*, 355. (c) Gorman, P. M.; Chakrabarty, A. *Biopolymers* **2001**, *60*, 381.
- (3) (a) Stockman, B. J.; Dalvit, C. *Prog. NMR Spectrosc.* **2002**, *41*, 187. (b) Palmer, A. G. *Chem. Rev.* **2004**, *104*, 3623. (c) Kay, L. E. *Biochem. Cell Biol.* **1998**, *76*, 145.
- (4) Hajduk, P. J.; Olejniczak, E. T.; Fesik, S. W. *J. Am. Chem. Soc.* **1997**, *119*, 12257.
- (5) Valensin, G.; Kushnir, T.; Navon, G. *J. Magn. Reson.* **1982**, *23*, 46.
- (6) Jarvet, J.; Damberg, P.; Bodell, K.; Goran Eriksson, L. E.; Graslund, A. *J. Am. Chem. Soc.* **2000**, *122*, 4261.
- (7) (a) Desvaux, H.; Berthault, P. *Prog. NMR Spectrosc.* **1999**, *35*, 295. (b) Desvaux, H.; Berthault, P.; Birlirakis, N.; Goldman, M. *J. Magn. Reson. A* **1994**, *108*, 219. (c) Bain, A. D.; Duns, G. J. *J. Magn. Reson. A* **1994**, *109*, 56.
- (8) Desvaux, H.; Goldman, M. *J. Magn. Reson. B* **1996**, *110*, 198.
- (9) Sklenar, V.; Piotto, M.; Leppik, R.; Saudek, V. *J. Magn. Reson. A* **1993**, *102*, 241.
- (10) Messerle, B. A.; Wider, G.; Otting, G.; Weber, C.; Wuthrich, K. *J. Magn. Reson.* **1989**, *85*, 608.
- (11) (a) Ramamoorthy, A.; Chandrakumar, N. *J. Magn. Reson.* **1992**, *100*, 60. (b) Cavanagh, J.; Fairbrother, W. J.; Palmer, A. G., III; Skelton, N. J. *Protein NMR: Principles and Practice*; Academic Press: London, 1996.
- (12) Mansfield, S. L.; Jayawickrama, D. A.; Timmons, J. S.; Larive, C. K. *Biochim. Biophys. Acta* **1998**, *1382*, 257.
- (13) (a) Tjernberg, L. O.; Naslund, J.; Lindqvist, F.; Karlstrom, A. R.; Thyberg, J.; Terenius, J.; Nordstedt, C. *J. Biol. Chem.* **1996**, *271*, 8545. (b) Wurth, C.; Guimard, N. K.; Hecht, M. H. *J. Mol. Biol.* **2002**, *319*, 1279.
- (14) (a) Paivio, A.; Jarvet, J.; Graslund, A.; Lannfelt, L.; Westlind-Danielsson, A. *J. Mol. Biol.* **2004**, *339*, 145. (b) Chiti, F.; Stefani, M.; Taddei, N.; Ramponi, G.; Dobson, C. M. *Nature* **2004**, *424*, 805.
- (15) (a) Mascioni, A.; Porcelli, F.; Ilangovan, U.; Ramamoorthy, A.; Veglia, G. *Biopolymers* **2003**, *69*, 29. (b) Ilangovan, U.; Ramamoorthy, A. *Biopolymers* **1998**, *45*, 9.

JA051714I